Using a Liquid Xenon Positron Target

Max Varverakis* and Robert Holtzapple†
California Polytechnic State University, San Luis Obispo, CA 93407, USA

Spencer Gessner‡
SLAC National Accelerator Laboratory, Menlo Park, California 94025, USA

Hiroki Fujii§
Nishina Center, RIKEN, 2-1 Hirosawa, Wako, Saitama, 351-0198, Japan
(Dated: August 10, 2022)

Colliding high energy electrons with a high-Z material – known as a positron target – is a common method for producing positrons for particle accelerator applications. The main consequence of using a solid positron target involves material degradation due to energy deposition from the beam, in which preventative measures require various techniques to dissipate thermal gains in the material. Rather than investigating the techniques to obviate the solid target problems, we explore the use a liquid Xenon positron target as an alternative to using solid targets. From simulations in GEANT4, we find that a liquid Xenon target has positron yields on the order of currently implemented solid targets while also maintaining comparable positron emittances and energies. With thoughtful design of a liquid Xenon chamber, we argue that one can more easily account for the energy deposits from the beam as compared to currently used solid targets.

I. INTRODUCTION

A common scheme for producing positrons is by colliding high energy electrons into a high-Z target. The collision between an electron beam and a solid target generates an electromagnetic particle shower, in which positrons are produced. Because the collision is such high energy, a great deal of energy is deposited in the target in the form of thermal energy. As a result, solid targets tend to degrade over time []. Since positron yield increases as a function of radiation length [], a thicker the target implies a greater positron yield, but that also implies a greater energy will deposited into the target, leading to a quicker degradation of the target.

There are various methods for increasing the life span of solid targets, such as using a cooling system [] and rotating the target so that the beam doesn't hit the same spot of the target every pulse [].

Previous experiments have been carried out to explore alternatives to using solid targets, such as using liquid Mercury (Hg), but the apparent hazards that Hg presents are too dangerous to implement in any efficient manner. Other approaches include...

For typical Linear Collider applications, around *** e^+ per second need to be produced [].

In this paper, we explore the possibility of using a liquid Xenon (Xe) target to produce positrons.

* mvarvera@calpoly.edu
† rholtzap@calpoly.edu
‡ sgess@slac.stanford.edu
§ hiroki.fujii@riken.jp

II. SIMULATION RESULTS

A. Comparing Liquid Xenon and Tantalum Targets

Comparison study between Tantalum (Ta) and liquid Xenon (lXe) because we have a reference study on Ta []. We used GEANT4 to simulate the collision between 10 GeV e^- and a target. We compare the results of using a Ta target and a lXe target.

See Table I for parameters used in the simulation.

Material	Z	Density [$g \cdot cm^{-3}$]	Radiation Length [cm]
Tantalum (Ta)	73	16.654	0.4094
Liquid Xe (lXe)	54	2.953	2.872

TABLE I: Parameters used in GEANT4 simulation when comparing targets.

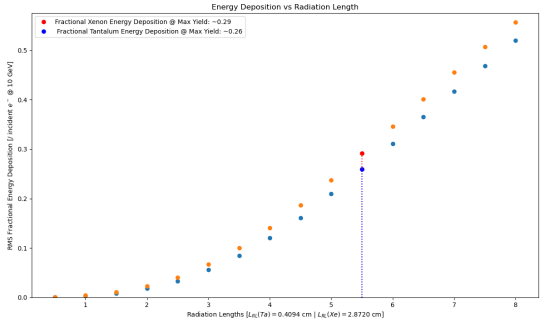

FIG. 1: Energy deposition in Ta and lXe targets per incident electron at 10 GeV.

1. *Calculating Positron Emittance*

To calculate the RMS emittance of the positrons generated in pair production, we utilize the following sets of equations []

$$\langle x^2 \rangle = \frac{\sum x^2}{n} - \left(\frac{\sum x}{n}\right)^2, \tag{1a}$$

$$\langle p_x^2 \rangle = \frac{\sum p_x^2}{n} - \left(\frac{\sum p_x}{n}\right)^2, \tag{1b}$$

$$\langle x p_x \rangle = \frac{\sum x p_x}{n} - \frac{\sum x \sum p_x}{n^2}, \tag{1c}$$

which gives us

$$\varepsilon_{n,rms} = \frac{1}{m_0 c}\sqrt{\langle x^2 \rangle \langle p_x^2 \rangle - \langle x p_x \rangle}. \tag{2}$$

Using these equations, we generate a plot of the x- and y-emittance of the positrons against target width for both Tantalum and liquid Xenon targets. As seen in Figure 2, both the x- and y-emittance of the positrons are lower in the Tantalum target than in the liquid Xenon target. According to [], the emittance values associated with liquid Xenon are still comparable for use in linear colliders.

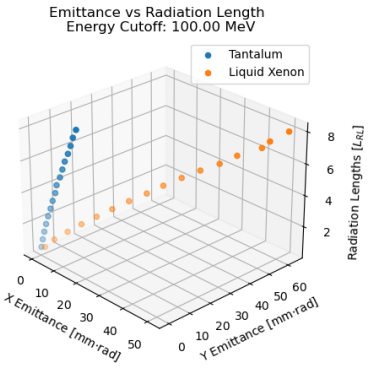

FIG. 2: Normalized RMS positron emittance in a Tantalum and liquid Xenon target for differing target widths. The positron energy cutoff was set to 100 MeV.

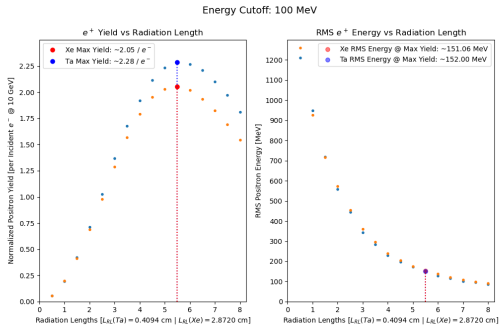

(a) Positron yield per incident electron at 10 GeV.

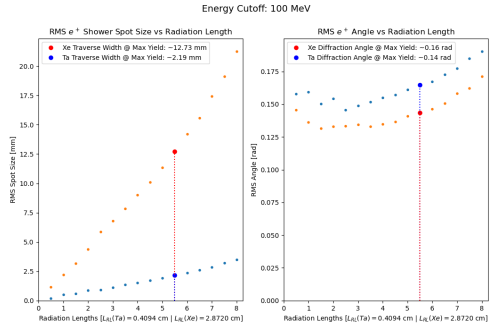

(b) Positron shower spot size and diffraction angle at the exit of the target.

FIG. 3: Positron yield per incident e^- at 10 GeV, shower spot size, and angular divergence of positrons upon exiting the target.

From Figure 3a, the max positron yield for both Ta and lXe occurs at around 2.75 radiation lengths. Despite having different radiation lengths, the energy of the positrons exiting the target at a given width are relatively equal for both target materials.

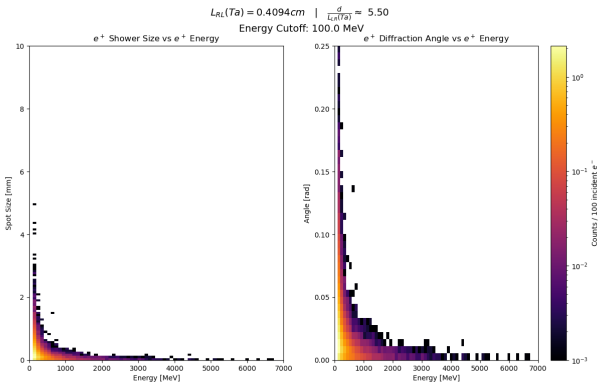

(a) Tantalum target.

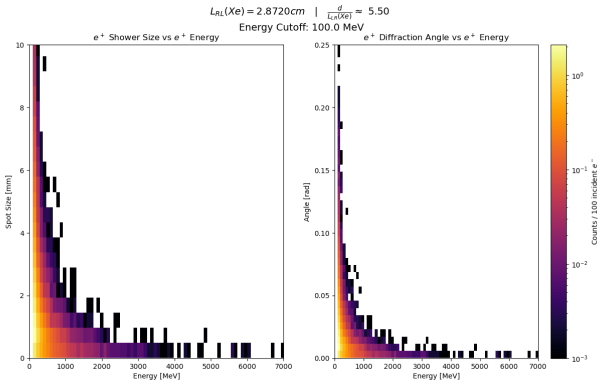

(b) Liquid Xenon target.

FIG. 4: Traverse width and angular diffraction of positrons as a function of their energy upon production. Data is shown for widths of 2.75 radiation lengths (max e^+ yield).

Notice that in Figure 4, the angular divergence of positrons is roughly the same for both targets, yet the traverse widths are more broadly distributed for the liquid Xenon target. This can be explained by the fact that the radiation length of liquid Xenon is roughly seven times that of Tantalum.

B. Setting a Cutoff Traverse Width

Although the max yield for liquid Xenon is on par with that of the Tantalum target according to Figures 3b and 4, the physical spread of positrons produced from the liquid Xenon target is much larger than that of the Tantalum target. As a result, only a fraction of the positrons that exit the target will have the right characteristics to make it down the rest of the accelerator. In order to accurately assess the plausibility of using a liquid Xenon positron target, we set cutoffs for the traverse width of positrons created during the collision.

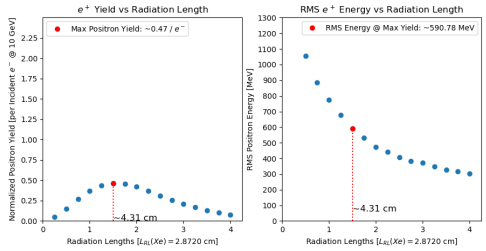

(a) 1 mm cutoff

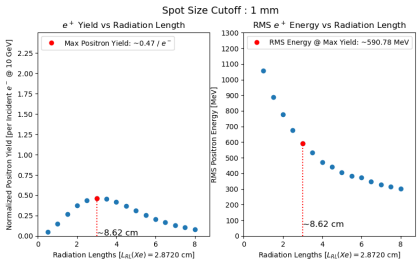

(b) 5 mm cutoff

FIG. 5: Positron yield and energy using a liquid Xenon target with a 1 mm and 5 mm traverse width cutoff.

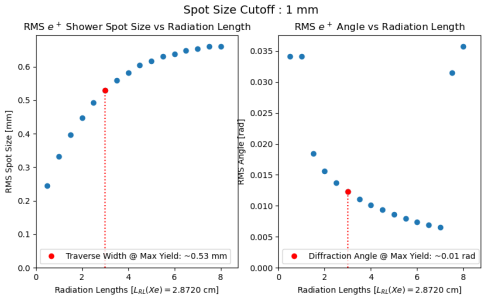

(a) 1 mm cutoff

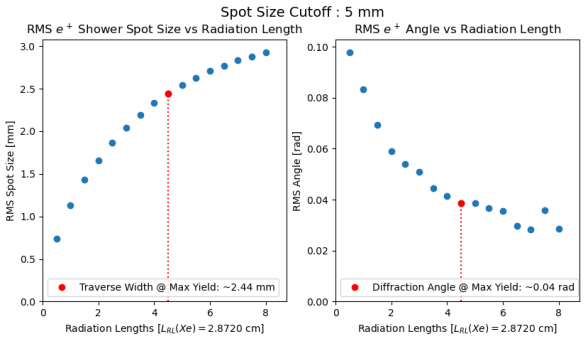

(b) 5 mm cutoff

FIG. 6: Positron spot size and angular diffraction using a liquid Xenon target with a 1 mm and 5 mm traverse width cutoff.

It is reassuring to see that even after removing the positrons from the dataset with large transverse distances from the beam path, there are still a comparable number of positrons that we predict will be able to make it to the

next stage of the accelerator [].

III. CRYO-COOLED LIQUID XENON CHAMBER

Figure 7, a basic schematic of how the liquid Xenon chamber will interact with the beam.

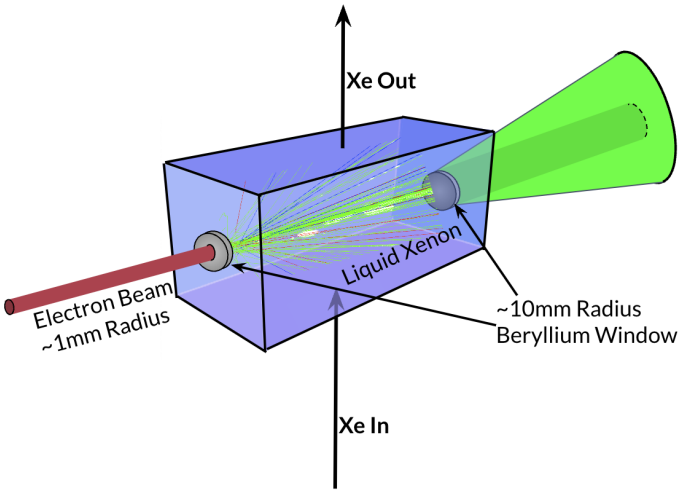

FIG. 7: Schematic of liquid Xenon setup.

A. Calculating the Liquid Xenon Flow Rate

To calculate the flow rate of the liquid Xenon, we first calculate preliminary values using the information given in the table below.

Liquid Xenon	Symbol	Value	Units
Molar Mass	M	131.293	u
Density	ρ	2.953	$g \cdot cm^{-3}$
Heat of Vaporization	ΔH	12.636	$kJ \cdot mol^{-1}$
Heat of Vap./Volume	ΔH_{vol}	284.205	$J \cdot cm^{-3}$
Radiation Length	L_{RL}	2.872	cm
Width	$\frac{d}{L_{RL}}$	5.5	L_{RL}

TABLE II: Important parameters associated with liquid Xenon target chamber.

We first convert the heat of vaporization to units of Joules per unit volume ($J \cdot cm^{-3}$), which is given by Eq. (3a). We then calculate the number of electrons per beam bunch (SLAC), by comparing the total charge of the beam bunch to the charge of an electron ($e \approx 1.602 \times 10^{-10}$ nC), as follows from Eq. (3b). From this, we calculate the total energy deposited in the liquid Xenon target, as seen in Eq. (3c).

$$\Delta H_{vol} = \frac{\Delta H \cdot \rho}{M}, \tag{3a}$$

$$n = \frac{q}{e}, \tag{3b}$$

$$\epsilon = n \cdot E_{dep}. \tag{3c}$$

Now we have everything we need in order to calculate the flow rate of liquid Xenon required to replace the vaporized Xenon due to the energy deposited by the beam,

$$Q = \frac{\epsilon \cdot f}{\Delta H_{vol}}. \tag{4}$$

In case one wants to calculate the flow rate required to move the entire volume encompassing the main part of the EM shower, one can approximate the volume with a rectangular prism with target width and other side lengths equal to the diameter of the Beryllium windows (see next section). At max positron yield, this gives $V = (2\text{ cm})^2 \cdot 5.5 L_{RL} \approx 63.18\text{ cm}^3$. As a result, the required flow rate to move volume V in the amount of time between beam pulses is shown in Table III as Q_{vol}.

B. Using Beryllium Windows to the Target Chamber

We explore using Beryllium windows for the beam to enter the target chamber. Below is some useful information about Beryllium.

Utilizing Bernoulli's Equation for conservative force fields [], we can calculate the total pressure on a Beryllium window, which is of the form

$$P = \frac{1}{2}\rho v^2 + \rho g h + p, \tag{5}$$

where v is the fluid flow rate, g is acceleration due to gravity, h is the height of the Xenon chamber relative to the height of the window, and p is the additional pressure from, say, the atmosphere. However, as seen in Table III, the flow rate for the liquid Xenon is quite small. Additionally, the liquid Xenon chamber is in vacuum, and we are comparing differences in total pressures, so we can ignore p as well. Therefore, we can ignore the second order term and the point-pressure term to further simplify our approximation to

$$P = \rho g h. \tag{6}$$

From Eq. (6), we can calculate the force on a Beryllium window with contact area A by multiplying the area by the pressure: $F = P \cdot A$.

In order to determine the required thickness of the Beryllium window, we utilize the following []. First we calculate a constant related to the safety factor of our thickness, which takes into account the method with

Beam Parameters	**Symbol**	**FACET-II**	**ILC**	**Units**
Energy	E	10.0	6.0	GeV
Repetition Rate	f	10	300	Hz
Charge	q	2	3.204	nC
Number of e^-	n	1.248	2.0	10^{10}
Resultant Quantities				
Energy Deposition/e^-	$\mathrm{E_{dep}}$	.66581		GeV
Energy Deposit/Pulse	ϵ	1.332	735.9	J
Energy Deposit Density	ϵ_ρ	1.63×10^{-3}	3.10	$\mathrm{J{\cdot}g^{-1}}$
Power Deposit	P_{dep}	3.86	7.359×10^8	W
Flow Rate due to Vaporization	Q	4.685×10^{-2}	776.8	$\mathrm{cm^3 \cdot s^{-1}}$
Main Shower Path Flow Rate	Q_{vol}	0.6318	18.96	$\mathrm{L{\cdot}s^{-1}}$

TABLE III: Linear collider electron beam parameters and associated target quantities [].

Beryllium	**Symbol**	**Value**	**Units**
Atomic Number	Z	4	
Density	ρ	1.844	$\mathrm{g{\cdot}cm^{-3}}$
Rupture Modulus	F_a	400	MPa
Quantities			
Height [a]	h	1.0	m
Radius	r	10.00	mm
Contact Area	A	100π	$\mathrm{mm^2}$
Pressure	P	28.968	kPa
Force	F	9.100	N
Safety Factor	S_F	4	
Empirical Constant	K	0.75	
Thickness	T	147.395	μm

[a] Difference in height between the Beryllium window and the top of the liquid Xenon chamber.

TABLE IV: Useful quantities and properties of solid Beryllium. The quantities are specific to a 10mm radius Beryllium disk.

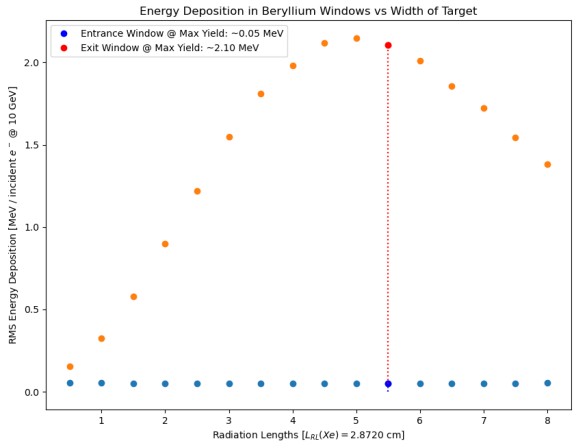

FIG. 8: Energy deposition on incident and exit Beryllium windows.

which the Beryllium window is inserted into the target chamber. An empirical constant $K = 0.75$ is chosen if the window is clamped into the target chamber, and $K = 1.125$ if the window is unclamped in the target chamber. For a given safety factor (S_F), we have a thickness of

$$T = r \cdot \sqrt{\frac{S_F \cdot K \cdot P}{F_a}}. \tag{7}$$

IV. CONCLUSION

A. Design of Liquid Xenon Chamber

Here we explore how one could design a chamber for the liquid Xenon target.

Source code and sample data for GEANT4 simulations can be found at `https://github.com/MaxVarverakis/LiquidXenonSims.git`.

ACKNOWLEDGMENTS

We wish to acknowledge the support of the author community in using REVTEX, offering suggestions and encouragement, testing new versions, ...

Appendix A: Appendixes

To start the appendixes, use the `\appendix` command. This signals that all following section commands refer to appendixes instead of regular sections. Therefore, the `\appendix` command should be used only once—to setup the section commands to act as appendixes. Thereafter normal section commands are used. The heading for a section can be left empty. For example,

```
\appendix
\section{}
```

will produce an appendix heading that says "APPENDIX A" and

```
\appendix
\section{Background}
```

will produce an appendix heading that says "APPENDIX A: BACKGROUND" (note that the colon is set automatically).

If there is only one appendix, then the letter "A" should not appear. This is suppressed by using the star version of the appendix command (`\appendix*` in the place of `\appendix`).

Appendix B: A little more on appendixes

Observe that this appendix was started by using

```
\section{A little more on appendixes}
```

Note the equation number in an appendix:

$$E = mc^2. \tag{B1}$$

1. A subsection in an appendix

You can use a subsection or subsubsection in an appendix. Note the numbering: we are now in Appendix B 1.

Note the equation numbers in this appendix, produced with the subequations environment:

$$E = mc, \tag{B2a}$$
$$E = mc^2, \tag{B2b}$$
$$E \gtrsim mc^3. \tag{B2c}$$

They turn out to be Eqs. (B2a), (B2b), and (B2c).